Received: 12 August 2019 | Revised: 22 January 2020 | Accepted: 27 January 2020

DOI: 10.1002/mrc.5003

SPECIAL ISSUE RESEARCH ARTICLE

WILEY

Valine derived poly (acetylenes) as versatile chiral lyotropic liquid crystalline alignment media for RDC-based structure elucidations

Alexis Krupp[1,2] | **Markus Noll**[1] | **Michael Reggelin**[1]

[1]Clemens Schöpf Institut for Organic Chemistry and Biochemistry, Technical University of Darmstadt, Darmstadt, Germany

[2]Nitrochemie Aschau GmbH, Aschau am Inn, Germany

Correspondence
Michael Reggelin, Clemens Schöpf Institut for Organic Chemistry and Biochemistry, Technical University of Darmstadt, Alarich-Weiss Straße 4, Darmstadt 64287, Germany.
Email: re@chemie.tu-darmstadt.de

Funding information
German Research Council (DFG), Grant/Award Number: FOR 934 (Re 1007/7-1); TECHNISCHE UNIVERSITAET DARMSTADT

Abstract

Anisotropic samples of lyotropic liquid crystalline (LLC) phases of valine derived polyaryl acetylenes were employed as chiral alignment media for the measurement of residual dipolar couplings (RDCs) of 12 small, chiral, organic molecules. The quadrupolar splitting of the deuterium signal of $CDCl_3$ can be adjusted by temperature and concentration changes from 0 to 350 Hz. The LLC phases showed excellent orienting properties for all analytes bearing various functional groups. The precise extraction of RDCs in the range of up to ±30 Hz from F2-coupled HSQC spectra was possible. Additionally, the chiral environment led to diastereomorphous interactions with the enantiomers of chiral analytes leading to two different sets of RDCs. This differential order effect was particularly pronounced with H-bond donors like alcohols and 2° amines.

KEYWORDS

computational chemistry, enantiodifferentiation, lyotropic liquid crystalline phases, NMR spectroscopy, polyacetylenes, residual dipolar couplings

1 | INTRODUCTION

The application of anisotropic NMR-parameters in structural analyses of molecules in solution has improved the quality of structure elucidations considerably.[1] A precondition for their measurement is to hinder the molecule under consideration from tumbling isotropically to such an extent that anisotropic interactions become measurable without complicating spectral analyses by strong coupling (*weak alignment*). In the case of residual dipolar couplings (RDCs) for a one-bond C–H coupling, this precondition is fulfilled when the medium scales the maximum dipolar coupling by roughly a factor of 1,000. This can be achieved by mainly two types of alignment media both having their merits and shortcomings. Stretched or compressed gels prepared by uniaxial swelling of crosslinked polymers (SAG: *strain induced alignment in a gel*)[2] have the advantage of facile scaling of the alignment strength, which frequently is counterbalanced by lengthy sample preparation procedures. Lyotropic liquid crystalline (LLC) phases[3] on the other hand offer fast and simple sample preparation (and sample recovery) but suffer from the existence of a critical concentration necessary for entering the anisotropic

[Correction added on 19 January 2021, after first online publication: The copyright line was changed.]

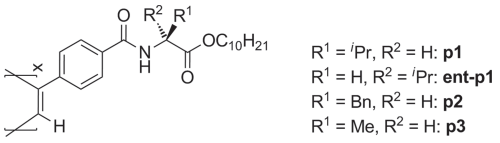

FIGURE 1 Poly (phenylacetylenes) applied as alignment media in RDC-based structure elucidations[7a, b, d]

state (c_{crit}). If this lowest possible concentration already orients the molecule too strong, then the extraction of residual anisotropic data is at least strongly hampered.

Nonetheless, in the last decade, both alternatives have been applied to an ever-increasing number of structural problems in which configurational problems played a dominant role.[1g, 4] This development was driven by successful work on new media being compatible with organic solvents and the exploitation of polymer classes beyond the homopolypeptides dominating the LLC phases for many years.[1v, 3i, k, 5] These efforts first led to the application of helically chiral polyguanidines[6] and later to polyaryl acetylenes with amino acid derived side chains as chiral alignment media (Figure 1).[7] The amino acid derived polyaryacetylenes have been developed mainly by Yashima[8] and Tang[9] among others to study fundamental aspects of dynamic helical polymers as well as possible applications as chiral resolving agents[8a, 10] or, more recently, as chiral polymeric catalysts.[11]

Encouraged by the very promising results using the valine and phenylalanine derived polymers **p1**/***ent*-p1** and **p2** *as enantiomer differentiating LLC phases* (moreover, **p2** has been used to elucidate the conformation of a calix[4]arene derivative by others),[12] we started to investigate the constitutional scope of their alignment properties. This included not only the variation of functional groups and the carbon skeleton of the compounds; it also addressed the interplay of these properties with the differential order effect. This work should be the basis for a deeper understanding of the alignment process in general and the enantiomer differentiating capability of the medium in particular. The knowledge gained from these studies will influence work directed towards the elucidation of absolute configurations from anisotropic NMR data. In the following, we would like to describe our results with the enantiomeric polymers **p1** and ***ent*-p1**.*

*In a strict sense, the two polymers are not enantiomers. They would be enantiomers if both polymers (with inverted absolute configuration at the repeating units and inverted helicity of the backbone) would contain the same number of repeating units, which is not exactly the case. Given the high molecular weight of the polymers, this difference can be neglected to a good approximation.

TABLE 1 Polymer data and critical concentration c_{crit}

Polymer	M_n[a] (10^5 g/mol)	$[\Theta]^{30°C\ b}_{368\ nm}$ (10^4·deg·cm^2·dmol^{-1})	c_{crit}[c] (%, w/w)
p1-a	9.08	4.28	13.6
p1-b	5.88	4.22	14.1
***ent*-p1-c**	3.25	−4.18	14.1
***ent*-p1-d**	1.46	−4.31	14.7

[a]Number of average molecular weight calibrated against polystyrene.
[b]Molar ellipticity.
[c]Critical concentration (w/w) for the phase transition.

2 | RESULTS AND DISCUSSION

As described earlier, the monomer synthesis can be achieved in a three step reaction sequence starting from the enantiomers of valine and 4-iodobenzoic acid ethyl ester.[7a] In the meantime, we improved and simplified the procedure increasing the overall yield from 56% to 71% (see Supporting Information).

Nine polymer preparations from the two enantiomeric monomers were synthesized. They were characterized by their molecular weight and chiroptical data (see Supporting Information). Moreover, for four selected polymers, we determined the critical concentration (c_{crit}) in $CDCl_3$ necessary to enter the anisotropic state (Table 1). After complete disappearance of the singlet from the isotropic phase, we determined the quadrupolar splitting ($\Delta\nu_Q$) of the deuterium solvent signal after the anisotropic state has been reached.†

Because polymer chains experience an alignment in a magnetic field due to their magnetic susceptibility, the phase morphology of the liquid crystal changes with time in the magnetic field.[3b, 13] This effect can be monitored by measuring time dependent ^{2}H-NMR spectra until no further change in the quadrupolar splitting is visible. For both, the time evolution of the quadrupolar splitting as well as the line width an equilibrium state can be observed after approximately 50 min.[14] For all NMR studies presented in the following, this period was waited at least to ensure full equilibration of the system.

To evaluate the homogeneity of the LLC phases after equilibration, a two-dimensional ^{2}H-imaging experiment published by Gil et al.[15] was used. As expected for solutions and in contrast to many gels, it could be demonstrated thereby that the homogeneity of the phase is very pronounced making it possible to extract the couplings in high accuracy with less than 1% deviation along the sample (Figure 2a). Motivated by the question to what extent

†For a video describing the preparation of the LLC phases, see https://www.youtube.com/watch?v=C8cNWgJViGw.

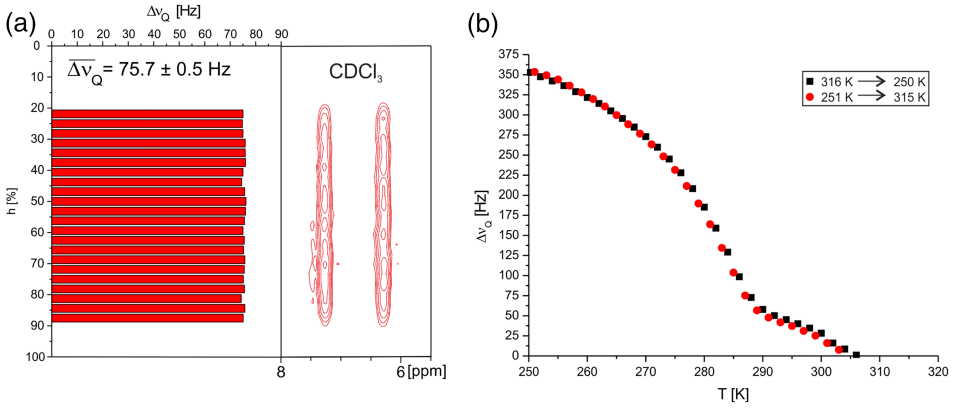

FIGURE 2 (a) Spatially resolved ^{2}H-NMR spectra of a 16.8% (w/w) sample of *ent*-**p1c** at 300 K. Note the perfect homogeneity of the sample. (b) Temperature dependence of the quadrupolar coupling of $CDCl_3$ in a LLC phase of **p1-e** at 14.6% (w/w). Black squares denote data points from cooling (316 K to 250 K), red circles from heating (251 K to 315 K)

it might be possible to scale the alignment strength by varying the temperature and considering the unusual temperature dependence of the induced orientation observed and utilized to generate multi alignment data sets in LLC phases of **p2**,[7b] we monitored the quadrupolar coupling constant in a temperature range for **p1** between 250 K and 316 K (Figure 2b). Starting with a 14.6% (w/w) solution at 316 K, no anisotropic phase is present denoted by the absence of a quadrupolar splitting. The anisotropic state is entered first at 306 K and increased by cooling the sample linearly with a slope of 3.5 Hz/K until 289 K. Below this temperature, the linear behavior is replaced by a nonlinear curve until 250 K. This change may indicate a change of the morphology of the LLC phase, which promised the opportunity to get an additional independent alignment tensor similar as has been observed with the LLC phases of **p2**.[7a, b] Therefore, a sample of **p1** containing (−)-IPC was measured at 300 K and 270 K, but unexpectedly, no significant difference of the corresponding tensors could be found. The measured RDCs scale approximately linear with the quadrupolar splitting of $CDCl_3$ at the two temperatures. Recent work in our group, focused on improvements in the polymer preparations, revealed that nonlinear temperature dependencies of the quadrupolar splitting occur preferentially when the polydispersity index of the polymer is high. Under better controlled conditions with a vinyl rhodium initiator, a linear or at least close to linear behavior is observed.[16]

To determine the scope and limitations of the suitability of LLC phases derived from valine based poly (phenylacetylenes) (PPAs) in structure elucidations of small organic compounds, we executed an extended study with 12 chiral analytes displaying various functional groups and varying degrees of conformational flexibility (Table 2 and Figure 3). The aim of the study was to address questions like phase compatibility with functional groups, alignment strength depending on molecular size and shape, capability of the phase to differentiate the enantiomers of chiral analytes, and finally to learn about the mechanisms of the orientation process. This latter point is not only important for the development of new media; it is surely one important aspect in efforts directed towards the determination of absolute configurations by NMR.

For the determination of the enantiodifferentiating capability of the phase, all analytes were measured under diastereomorphic conditions meaning that either both enantiomers of the analyte were measured at constant absolute configuration of the LLC phase or the measurements were performed in LLC phases of opposite absolute configuration (*heterochiral comparison*) at constant analyte configuration. The (obvious)[‡] validity of this approach to get equivalent diastereomorphic alignment data sets from analytes available only in one absolute configuration has been proven with the enantiomers of IPC and LLC phases derived from **p1**/***ent*-p1**.[7a]

All total coupling constants $^1T_{CH}$ were extracted from CLIP/CLAP-HSQC spectra[18] and were used to calculate the one-bond RDCs ($^1T_{CH} = {}^1J_{CH} + 2\ {}^1D_{CH}$). The couplings together with a structure model were used as input data for our newly developed program ConArch$^+$,[19] which uses a singual value decomposition (SVD)-based[20] method to calculate the alignment tensors and, if needed, distance geometry as structure generator in floating chirality calculations.

It is worth mentioning that the alignment strength is scalable over a wide range, either by changing the polymer concentration or, much more convenient, simply by a temperature change (Figures 2 and 3). Moreover, methods exist that allow for the precise measurement of large RDCs in LLC phases.[21]

For example, spectra of the fructose acetonide (#3 in Table 2) obtained from a 15.7% (w/w) LLC phase of *ent*-**p1c** at 300 K ($\Delta\nu_Q$ = 64 Hz) displayed broad lines preventing the extraction of couplings. Increasing the temperature to 310 K lowered the alignment strength significantly ($\Delta\nu_Q$ = 31 Hz), which allowed a precise

[‡]Imagine only the dextrorotatory analyte is available and we start with a P-helical phase, then the missing combination (−)-analyte /P-helix can be replaced by the enantiomorphic (+)-analyte/M-helix combination.

TABLE 2 Properties and NMR data of the oriented analytes

#[a]	Analyte[a]	Heterochiral combination	$\Delta\nu_Q$ (Hz)[b]	RDC range[exp] (Hz)	|maxRDC|[theo] (Hz)	maxRDC[theo] (% of $\Delta\nu_Q$)[b]	GDO (10^{-4})[b,d]	Dipole moment (D)	GCB[c]
1	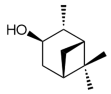 IPC	(−)|**p1**/(+)|**p1**	75/67[2)]	−23.8–15.2/−16.6–13.0	27.64/19.77	36.9/29.5[2)]	11.94/9.21[2)]	1.88	0.02
2	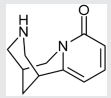 Cytisine	(−)|**p1**/(−)|*ent*-**p1**	81/80[1)]	−15.8–19.8/−31.0–7.4	27.32/32.45	33.7/40.6[1)]	11.81/14.22[1)]	7.40	0.49
3	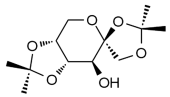 Fructose acetonide	(−)|**p1**/(−)|*ent*-**p1**	36/33[1)]	−9.8–18.9/−9.3–16.6	25.65/21.21	71.25/64.27	11.46/9.76[1)]	2.66	0.63
4	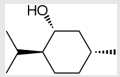 Menthol	(−)|**p1**/(−)|*ent*-**p1**	62/74[1)]	−4.9–18.7/−2.8–21.05	39.56/40.79	63.80/55.12	17.99/19.10[1)]	2.00	0.82
5	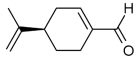 Perilla aldehyde	(−)|**p1**/(−)|*ent*-**p1**	54/34[1)]	−8.4–10.0/−7.6–7.1	16.37/14.19	30.30/41.74	7.41/6.57[1)]	n.d.	0.82
6	 α-Pinene	(−)|**p1**/(−)|*ent*-**p1**	85/89[1)]	−7.3–3.2/−8.1–3.5	8.27/9.65	9.73/10.84	3.98/4.55[1)]	0.27	0.95
7	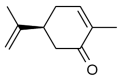 Carvone	(−)|*ent*-**p1**/(+)|*ent*-**p1**	70/63[3)]	−14.3–5.7/−9.0–7.4	18.01/14.12	25.73/22.41	9.25/6.16[3)]	4.52	0.95

(Continues)

TABLE 2 (Continued)

#[a]	Analyte[a]	Heterochiral combination	$\Delta\nu_Q$ (Hz)[b]	RDC range[exp] (Hz)	|maxRDC|[theo] (Hz)	maxRDC[theo] (% of $\Delta\nu_Q$)[b]	GDO (10^{-4})[b,d]	Dipole moment (D)	GCB[c]
8	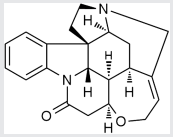 Strychnine	(−)|**p1**/(−)|*ent*-**p1**	57/54[1)]	−14.9–28.1/−11.7–21.5	29.19/20.84	51.21/38.59	13.98/9.74[1)]	4.32	0.97
9	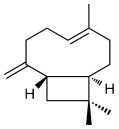 β-Caryophyllene	(−)|**p1**/(−)|*ent*-**p1**	110/102[1)]	−12.9 to −0.8/−11.5 to −0.4	34.00/28.91	30.90/28.34	14.64/12.41[1)]	0.53	0.98
10	 Camphor	(−)|**p1**/(+)|**p1**	81/73[2)]	−4.8–11.8/−4.8–10.9	12.01/11.29	14.83/15.47	5.20/4.94[2)]	4.13	0.99
11	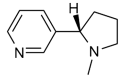 Nicotine	(−)|**p1**/(−)|*ent*-**p1**	56/57[1)]	−12.5–11.7/−14.8–13.2	25.33/29.74	45.23/52.18	10.88/12.76[1)]	3.51	0.99
12	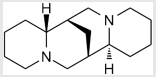 Sparteine	(−)|**p1**/(−)|*ent*-**p1**	96/95[1)]	−18.4–24.4/−16.5–25.3	27.64/29.23	28.79/30.77	13.13/13.56[1)]	0.90	0.99

[a]For exact sample compositions, measurement conditions, and detailed lists of measured couplings and results, see the Supporting Information.

[b]The quadrupolar splitting of the solvent, the GDO for the heterochiral combinations as well as the ratio of the largest RDC to the quadrupolar splitting are encoded as follows: 1) (−)-analyte-**p1**/(−)-analyte-*ent*-**p1**; 2) (−)-analyte-**p1**/(+)-analyte-**p1**; 3) (−)-analyte-*ent*-**p1**/(+)-analyte-*ent*-**p1**. For the actually used polymer batch (a–i), see the Supporting Information.

[c]GCB: "generalized cosine beta." The cosine of the intertensor angle for the heterochiral combinations.[17]

[d]GDO: "generalized degree of order."[17a]

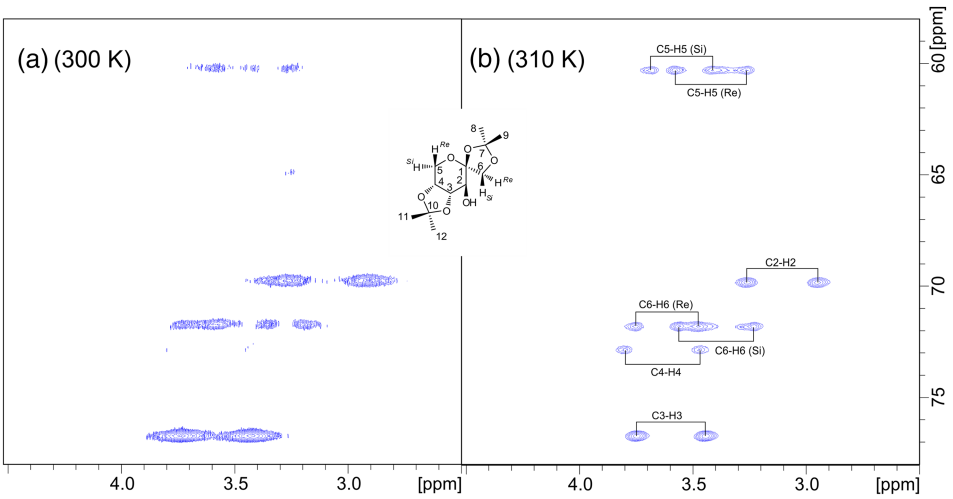

FIGURE 3 (a) Part of 500 MHz CLIP-HSQC spectrum of fructoseacetonide in a 15.7% (w/w) LLC phase of *ent*-**p1c** at 300 K in $CDCl_3$ ($\Delta\nu_Q = 64$ Hz). Severe line broadening hampers the extraction of coupling constants. (b) After raising the temperature from 300 K to 310 K, the quadrupolar splitting was reduced to 31 Hz improving the spectral quality considerably

analysis of the spectrum. The same effect can be achieved when the sample is diluted. At a polymer concentration of 14.5% (w/w), the splitting is again $\Delta\nu_Q = 31$ Hz but this time at 300 K.

As a first result, it can be stated that the LLC phases of **p1** and *ent*-**p1** are compatible with all analytes studied. With a few exceptions, most of the signals allowed the extraction of $^1T_{CH}$ with high accuracy. Therefore, for all structures, we achieved a satisfactory match between the measured and the back-calculated RDCs (see Supporting Information for details). For the rigid structures (pinene, β-caryophyllene, IPC, menthol, camphor, fructose acetonide, strychnine, and cytisine), it was sufficient to use a *single conformer single tensor* fit. Compounds with more conformational flexibility (carvone, perilla aldehyde, sparteine, and nicotine) were treated as conformational ensembles in *multi conformer single tensor* fits.[19,22]

2.1 | Orientational behavior

The results of the measurements are compiled in Table 2. We used both the general degree of order (GDO)[17a] and the relation between the largest possible RDC as calculated from the alignment tensor and the quadrupolar splitting of the solvent (*reduced RDC*^{max}) as measures for the ordering strength.

As expected, the hydrocarbons (#6 and #9) get oriented less as compared with all other compound classes, although the ketones (#7 and #10) are not far off. This means that for these compounds, a stronger orienting medium (higher $\Delta\nu_Q$) is necessary to generate RDCs in the favorable range of 5–20 Hz. Given the fact that all compounds studied are different in all aspects of their structures (e.g., different in shape, functional groups, H-bonding capabilities, and dipole moment), it is not straightforward to correlate these molecular properties with the mode of their orientation. One even may discuss the possibility that the specific interactions with the polymer may be superimposed by interactions with the oriented solvent. This would mean that the analytes orientation is a consequence of their interaction with the short-range ordered helices of the polymer strands surrounded by a chirally oriented solvent shell. The existence of the latter has been shown for dimethyl sulfoxide as solvent and a closely related polyacetylene.[23] Moreover, such chiral solvent imprints (chiral microsolvation) have been observed several times before in the context of optical rotatory dispersion (ORD) calculations.[24]

2.2 | Enantiodifferentiation

The phases used in this study are chiral. They display a *P*-helical chain that is *S*-configured and vice versa.[§] This chirality causes the LLC phases derived from these polymers to be chiral too, which in turn leads to the diastereomorphic interactions with chiral analytes as already mentioned and shown in 2012[7a] and 2019.[16a] In the latter publication, it was demonstrated by ^{2}H-RQC measurements in natural abundance that **p1** is even able to differentiate the enantiomers of 3-methyl hexane in an unprecedented scale (17 out of 20 possible quadrupolar doublets have been observed). In the context of any efforts directed towards the determination of absolute configurations of dissolved molecules by anisotropic NMR, the maximization of the differential order effect[25] for the enantiomers of a given analyte is a major goal. Therefore, we extended our investigation to explore the enantiodifferentiating capability of the phases and to learn something about the factors governing this capability. As discussed earlier, the terms "enantiodifferentiation"

[§]Although there is no study in the literature describing the helical assignment of **p1** as such, there is evidence for the correctness of this assignment based on refs.[9d] and.[8g]

or "enantiomer differentiation" are used to describe any heterochiral combination between the phase and the analyte in which, for example, the combinations (+) and (−)-analyte with P-helical polymer is equivalent to, for example, (+)-analyte with P and M-helical polymer. As a quantitative measure to describe the enantiodifferentiation (or to be more precise: the enantiomer differentiating *orientation*), we used the cosine of the intertensor angle (generalized cosine beta [GCB])[17b] of the alignment tensors calculated for the heterochiral combinations under consideration (Table 2 and Figure 4). This entails that low GCB values (close to 0) mean a high enantiodifferentiation and high values (close to 1) the opposite.

A closer look at Table 2 and Figure 5 implies that a large difference in the *general degree of order related to the quadrupolar splitting* (GDO/$\Delta\nu_Q$) of the enantiomers (or equivalent heterochiral combination) is a necessary but not sufficient precondition for a good differentiation in terms of differential *orientation.*

Obviously and as expected, some specific interaction with the chiral polymer is needed to achieve enantiodifferentiation. There are five analytes with good to excellent differentiation (#1–5 in Table 2). Four of them are H-bond donors (three alcohols and one 2° amine). The fifth of the highly differentiated compounds is perilla aldehyde, which may interact with the polymer in its dienol form, thus being also an H-bond donor.[26] The hydrocarbons pinene and caryophyllene, the 3° amine sparteine, and the ketone camphor behave as expected with a low enantiodifferentiation correlating to a small GDO/$\Delta\nu_Q$ difference. On the other hand, despite

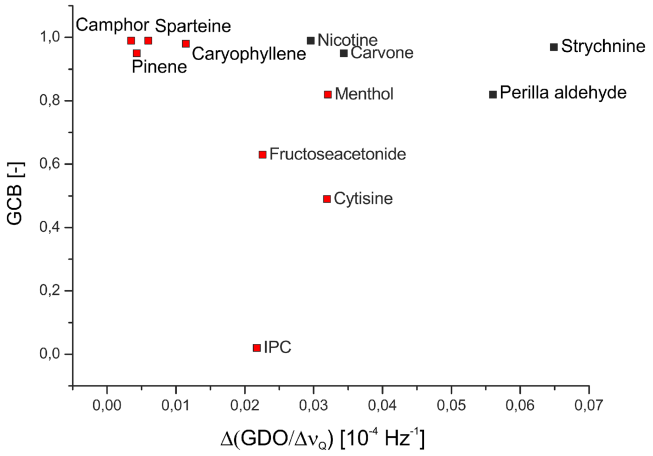

FIGURE 5 Dependence of the enantiodifferentiating orientation (GCB) on the reduced ordering difference (GDO/$\Delta\nu_Q$) of the heterochiral combinations

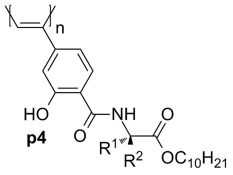

FIGURE 6 Possible structure of a hydrogen bonding donor functionalized polyaryl acetylene

the fact that the 3° amine nicotine and the ketone carvone display quite large GDO/$\Delta\nu_Q$ differences, their enantiodifferentiating orientation is neglectable. An extreme case is strychnine with the largest Δ (GDO/$\Delta\nu_Q$)

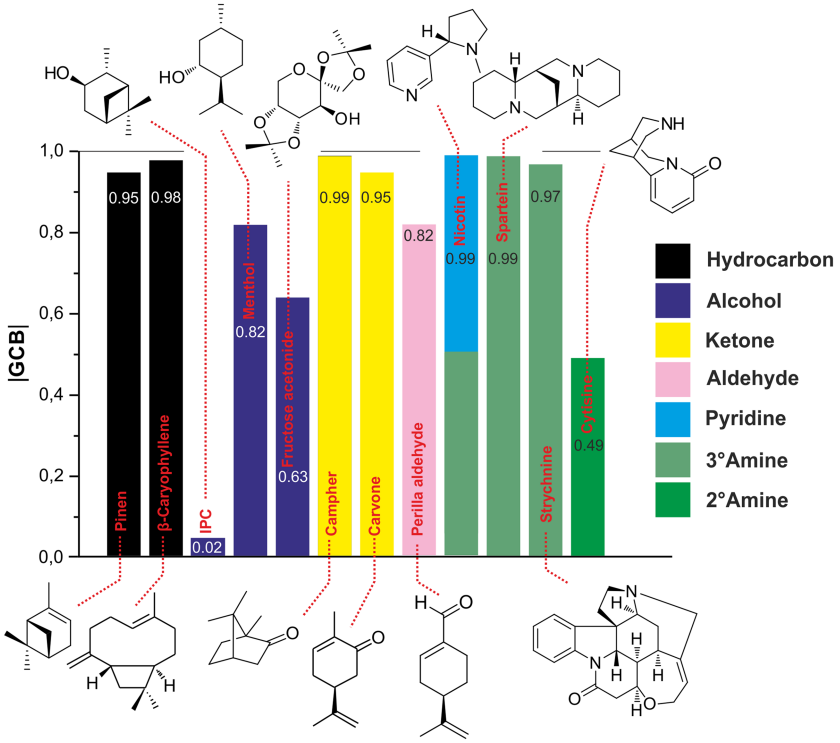

FIGURE 4 Graphical illustration of the generalized cosine β (GCB) values derived from the measurements of 12 analytes

and almost no differential ordering. This latter case is especially difficult to discuss, because of the many possible factors influencing its orientational behavior (molecular shape, functional groups, and dipole moment). The inverted situation, a small GDO difference but a good enantiodifferentiation was not observed, although there is no principal reason why this may not be the case for some other analyte. Finally, it should be mentioned that the GCB values for IPC in PBLG or PELG are much smaller (0.99 and 0.87, respectively) as compared with the ones in **p1**.[5g]

3 | CONCLUSIONS

In conclusion, we have shown that chiral LLC phases prepared by dissolving helically chiral valine derived polyaryl acetylenes in deuterated chloroform are compatible with 12 different analytes (Figure 4). These compounds cover a wide range of functional groups (olefins, alcohols, aldehydes, ketones, amides, 2°, and 3° amines) and differ considerably in their dipole moments and molecular shape. The analysis of their GDO related to a variable that expresses the maximum measured RDC in relation to the quadrupolar splitting of the solvent (reduced RDC^{max}) led to the idea that the orientation of the solvent may be an important driving force for the orientation of the analytes. The data obtained from the RDC-analysis of the heterochiral combinations suggest the guess that enantiodifferentiating orientation scales with the difference in the GDO for the heterochiral combinations as a necessary but not sufficient precondition. Maximum enantiodifferentiation has been achieved with H-bond donating alcohols and 2° amines. For easy enolizable aldehydes (and maybe ketones as well) like perilla aldehyde, we propose that the enol form plays an important role in the interaction with the phase. Guided by the obviously important role of H-bonding in the chiral recognition process, we are currently investigating the phenolic polymers **p4** as H-bond donors being kind of "umpoled" systems to differentiate H-bond acceptors like ketones that are not sensitive to **p1** (Figure 6).

EXPERIMENTAL SECTION

Experimental details for the monomer, polymer, and phase preparations as well as sample compositions can be found in the Supporting Information. Moreover, characterization data (CD spectra, ORD, and NMR data) and tensor calculations can be found there.

ACKNOWLEDGEMENTS

The authors would like to thank the German Research Council (DFG) for funding of the Research Unit FOR 934 (RE 1007/7-1). Special thanks to Dr. S. Immel for the tensor calculations with ConArch^{+}.[19]

Open Access funding enabled and organized by Projekt DEAL.

ORCID

Michael Reggelin https://orcid.org/0000-0003-3650-3921

REFERENCES

[1] a) Y. Liu, A. Navarro-Vázquez, R. R. Gil, C. Griesinger, G. E. Martin, R. T. Williamson, *Nat. Protoc.* **2019**, *14*, 217; b) A. Navarro-Vázquez, R. R. Gil, K. Blinov, *J. Nat. Prod.* **2018**, *81*, 203; c) N. Marcó, R. R. Gil, T. Parella, *Magn. Reson. Chem.* **2017**, *55*, 540; d) Y. Liu, J. Saurí, E. Mevers, M. W. Peczuh, H. Hiemstra, J. Clardy, G. E. Martin, R. T. Williamson, *Science* **2017**, *356*, 43; e) L. Castañar, M. Garcia, E. Hellemann, P. Nolis, R. R. Gil, T. Parella, *J. Org. Chem.* **2016**, *81*, 11126; f) R. R. Gil, C. Griesinger, A. Navarro-Vázquez, H. Sun, *Structure Elucidation in Organic Chemistry: The Search for the Right Tools*, Wiley-VCH, Weinheim **2015** 279; g) R. R. Gil, C. Griesinger, A. Navarro-Vázquez, H. Sun, *Structure Elucidation in Organic Chemistry*, Wiley-VCH Verlag GmbH & Co. KGaA, New York **2015** 279; h) B. Böttcher, C. M. Thiele, *eMagRes*, John Wiley & Sons, Ltd, Chichester, UK **2012** 169; i) P. Trigo-Mouriño, A. Navarro-Vázquez, J. F. Ying, R. R. Gil, A. Bax, *Angew. Chem. Int. Ed.* **2011**, *50*, 7576; j) G. Kummerlöwe, B. Crone, M. Kretschmer, S. F. Kirsch, B. Luy, *Angew. Chem. Int. Ed.* **2011**, *50*, 2643; k) B. Luy, *J. Indian Inst. Sci.* **2010**, *90*, 119; l) C. Gayathri, M. C. de la Fuente, B. Luy, R. R. Gil, A. Navarro-Vázquez, *Chem. Commun.* **2010**, *46*, 5879; m) G. Kummerlöwe, B. Luy, in *Annu. Rep. NMR Spectrosc., Vol. 68* (Ed.: G. A. Webb), **2009**, pp. 193-230; n) G. Kummerlöwe, B. Luy, *TrAC Trends Anal. Chem.* **2009**, *28*, 483; o) M. E. García, S. Pagola, A. Navarro-Vázquez, D. D. Phillips, C. Gayathri, H. Krakauer, P. W. Stephens, V. E. Nicotra, R. R. Gil, *Angew. Chem. Int. Ed.* **2009**, *48*, 5670; p) C. M. Thiele, *Eur. J. Org. Chem.* **2008**, 5673; q) G. W. Li, H. Liu, F. Qiu, X. J. Wang, X. X. Lei, *Nat. Product. Bioprospecting* **2018**, *8*, 279; r) G. Cornilescu, R. F. R. Alvarenga, T. P. Wyche, T. S. Bugni, R. R. Gil, C. C. Cornilescu, W. M. Westler, J. L. Markley, C. D. Schwieters, *ACS Chem. Biol.* **2017**, *12*, 2157; s) E. Troche-Pesqueira, C. Anklin, R. R. Gil, A. Navarro-Vázquez, *Angew. Chem. Int. Ed.* **2017**, *56*, 3660; t) P. Tzvetkova, B. Luy, S. Simova, *Magn. Reson. Chem.* **2012**, *50*, S92; u) R. R. Gil, *Angew. Chem. Int. Ed.* **2011**, *50*, 7222; v) C. M. Thiele, *J. Org. Chem.* **2004**, *69*, 7403; w) L. Verdier, P. Sakhaii, M. Zweckstetter, C. Griesinger, *J. Magn. Reson.* **2003**, *163*, 353; x) R. R. Gil, *Residual Dipolar Couplings in Small-Molecule NMR*, Academic Press Ltd-Elsevier Science Ltd, London **2017**.

[2] a) Y. Z. Liu, A. Navarro-Vázquez, R. R. Gil, C. Griesinger, G. E. Martin, R. T. Williamson, *Nat. Protoc.* **2019**, *14*, 217; b) D. S. Carvalho, D. G. B. da Silva, F. Hallwass, A. Navarro-Vázquez, *J. Magn. Reson.* **2019**, *302*, 21; c) R. R. Gil, C. Gayathri, N. V. Tsarevsky, K. Matyjaszewski, *J. Org. Chem.* **2008**, *73*, 840; d) G. Kummerlöwe, J. Auernheimer, A. Lendlein, B. Luy, *J. Am. Chem. Soc.* **2007**, *129*, 6080; e)

J. C. Freudenberger, P. Spiteller, R. Bauer, H. Kessler, B. Luy, *J. Am. Chem. Soc.* **2004**, *126*, 14690; f) Chiral gels:T. Montag, C. Thiele, *Chem. A Eur. J.* **2013**, *19*, 2271; g) M. Schmidt, H. Sun, A. Leonov, C. Griesinger, U. M. Reinscheid, *Magn. Reson. Chem.* **2012**, *50 Suppl 1*, S38; h) G. Kummerlöwe, M. U. Kiran, B. Luy, *Chem. A Eur. J.* **2009**, *15*, 12192.

[3] a) I. E. Ndukwe, X. Wang, I. Pelczer, M. Reibarkh, R. T. Williamson, Y. Liu, G. E. Martin, *Chem. Commun.* **2019**, *55*, 4327; b) S. Jeziorowski, C. M. Thiele, *Chem. A Eur. J.* **2018**, *24*, 15631; c) M. Schwab, V. Schmidts, C. M. Thiele, *Chem. A Eur. J.* **2018**, *24*, 14373; d) M. Reller, S. Wesp, M. R. M. Koos, M. Reggelin, B. Luy, *Chem. A Eur. J.* **2017**, *23*, 13351; e) X. X. Lei, Z. Xu, H. Sun, S. Wang, C. Griesinger, L. Peng, C. Gao, R. X. Tan, *J. Am. Chem. Soc.* **2014**, *136*, 11280; f) P. Lesot, J. Courtieu, *Prog. Nucl. Magn. Reson. Spectrosc.* **2009**, *55*, 128; g) C. M. Thiele, *Concepts Magn. Reson. Part A* **2007**, *30A*, 65; h) P. Lesot, M. Sarfati, J. Courtieu, *Chem. A Eur. J.* **2003**, *9*, 1724; i) C. Aroulanda, V. Boucard, F. Guibe, J. Courtieu, D. Merlet, *Chem. A Eur. J.* **2003**, *9*, 4536; j) D. Merlet, B. Ancian, J. Courtieu, P. Lesot, *J. Am. Chem. Soc.* **1999**, *121*, 5249; k) I. Canet, J. Courtieu, A. Loewenstein, A. Meddour, J. M. Pechine, *J. Am. Chem. Soc.* **1995**, *117*, 6520; l) A. Meddour, I. Canet, A. Loewenstein, J. M. Pechine, J. Courtieu, *J. Am. Chem. Soc.* **1994**, *116*, 9652; m) J. P. Bayle, J. Courtieu, E. Gabetty, A. Loewenstein, J. M. Pechine, *New J. Chem.* **1992**, *16*, 837; n) D. B. DuPré, S. J. Yang, *J. Chem. Phys.* **1991**, *94*, 7466; o) W. Zong, G. W. Li, J. M. Cao, X. X. Lei, M. L. Hu, H. Sun, C. Griesinger, R. X. Tan, *Angew. Chem. Int. Ed.* **2016**, *55*, 3690; p) X. X. Lei, F. Qiu, H. Sun, L. W. Bai, W. X. Wang, W. S. Xiang, H. P. Xiao, *Angew. Chem. Int. Ed.* **2017**, *56*, 12857; q) G. W. Li, J. M. Cao, W. Zong, L. Hu, M. L. Hu, X. X. Lei, H. Sun, R. X. Tan, *Chem. A Eur. J.* **2017**, *23*, 7653.

[4] a) J. A. A. França, A. Navarro-Vázquez, X. Lei, H. Sun, C. Griesinger, F. Hallwass, *Magn. Reson. Chem.* **2017**, *55*, 297; b) N. Nath, E. J. d'Auvergne, C. Griesinger, *Angew. Chem. Int. Ed.* **2015**, *54*, 12706; c) A. Schütz, T. Murakami, N. Takada, J. Junker, M. Hashimoto, C. Griesinger, *Angew. Chem. Int. Ed.* **2008**, *47*, 2032.

[5] a) K. Czarniecka, E. T. Samulski, *Mol. Cryst. Liq. Cryst.* **1981**, *63*, 205; b) M. D. Poliks, Y. W. Park, E. T. Samulski, *Mol. Cryst. Liq. Cryst.* **1987**, *153*, 321; c) C. Aroulanda, M. Sarfati, J. Courtieu, P. Lesot, *Enantiomer* **2001**, *6*, 281; d) A. Meddour, P. Berdague, A. Hedli, J. Courtieu, P. Lesot, *J. Am. Chem. Soc.* **1997**, *119*, 4502; e) A. Marx, V. Schmidts, C. M. Thiele, *Magn. Reson. Chem.* **2009**, *47*, 734; f) V. Madiot, P. Lesot, D. Gree, J. Courtieu, R. Gree, *Chem. Commun.* **2000**, 169; g) S. Hansmann, T. Larem, C. M. Thiele, *Eur. J. Org. Chem.* **2016**, *7*, 1324.

[6] a) L. Arnold, A. Marx, C. Thiele, M. Reggelin, *Chem. A Eur. J.* **2010**, *16*, 10342; b) J. G. Kennemur, B. M. Novak, *Polymer* **2011**, *52*, 1693.

[7] a) N.-C. Meyer, A. Krupp, V. Schmidts, C. M. Thiele, M. Reggelin, *Angew. Chem. Int. Ed.* **2012**, *51*, 8334; b) A. Krupp, M. Reggelin, *Magn. Reson. Chem.* **2012**, *50*, S45; c) M. Dama, S. Berger, *Tetrahedron Lett.* **2012**, *53*, 6439; d) A. Krupp, *Ph.D.*, Technical University Darmstadt (Germany) **2015**.

[8] a) E. Yashima, K. Maeda, H. Iida, Y. Furusho, K. Nagai, *Chem. Rev.* **2009**, *109*, 6102; b) E. Yashima, K. Maeda, Y. Furusho, *Acc. Chem. Res.* **2008**, *41*, 1166; c) E. Yashima, K. Maeda, *Macromolecules* **2008**, *41*, 3; d) K. Maeda, E. Yashima, *Top. Curr. Chem.* **2017**, *375*, 31; e) K. Maeda, K. Shimomura, T. Ikai, S. Kanoh, E. Yashima, *Macromolecules* **2017**, *50*, 7801; f) E. Yashima, N. Ousaka, D. Taura, K. Shimomura, T. Ikai, K. Maeda, *Chem. Rev.* **2016**, *116*, 13752; g) K. Okoshi, S. Sakurai, S. Ohsawa, J. Kuniaki, E. Yashima, *Angew. Chem. Int. Ed.* **2006**, *45*, 8173.

[9] a) K. K. L. Cheuk, B. S. Li, J. W. Y. Lam, Y. Xie, B. Z. Tang, *Macromolecules* **2008**, *41*, 5997; b) J. Z. Liu, J. W. Y. Lam, B. Z. Tang, *Chem. Rev.* **2009**, *109*, 5799; c) J. W. Y. Lam, B. Z. Tang, *Acc. Chem. Res.* **2005**, *38*, 745; d) L. M. Lai, J. W. Y. Lam, B. Z. Tang, *J. Polym. Sci., Part A: Polym. Chem.* **2006**, *44*, 2117.

[10] a) C. Zhang, H. Wang, Q. Geng, T. Yang, L. Liu, R. Sakai, T. Satoh, T. Kakuchi, Y. Okamoto, *Macromolecules* **2013**, *46*, 8406; b) E. Yashima, H. Iida, Y. Okamoto, in *Differentiation of Enantiomers I*, (Ed: V. Schurig) Vol. 340, Springer-Verlag Berlin, Berlin **2013** 41; c) Y. Naito, Z. L. Tang, H. Iida, T. Miyabe, E. Yashima, *Chem. Lett.* **2012**, *41*, 809.

[11] a) L. M. S. Takata, H. Iida, K. Shimomura, K. Hayashi, A. A. dos Santos, E. Yashima, *Macromol. Rapid Commun.* **2015**, *36*, 2047; b) H. Iida, Z. L. Tang, E. Yashima, *J. Polym. Sci., Part A: Polym. Chem.* **2013**, *51*, 2869.

[12] L. Vrzal, K. Flidrova, T. Tobrman, H. Dvorakova, P. Lhotak, *Chem. Commun.* **2014**, *50*, 7590.

[13] a) M. Panar, W. D. Phillips, *J. Am. Chem. Soc.* **1968**, *90*, 3880; b) T. Kimura, *Polymer Journal* **2003**, *35*, 823; c) S. Sakurai, *Polymer* **2008**, *49*, 2781.

[14] P. Lesot, P. Berdagué, A. Meddour, A. Kreiter, M. Noll, M. Reggelin, *ChemPlusChem* **2019**, *84*, 144.

[15] P. Trigo-Mourino, C. Merle, M. R. M. Koos, B. Luy, R. R. Gil, *Chem. A Eur. J.* **2013**, *19*, 7013.

[16] a) P. Lesot, P. Berdague, A. Meddour, A. Kreiter, M. Noll, M. Reggelin, *ChemPlusChem* **2019**, *84*, 144; b) A. Kreiter, *Ph. D*, Technical University Darmstadt (Germany), **2017**.

[17] a) F. Kramer, M. V. Deshmukh, H. Kessler, S. J. Glaser, *Concepts Magn. Reson., Part A* **2004**, *21A*, 10; b) J. Sass, F. Cordier, A. Hoffmann, M. Rogowski, A. Cousin, J. G. Omichinski, H. Löwen, S. Grzesiek, *J. Am. Chem. Soc.* **1999**, *121*, 2047.

[18] A. Enthart, J. C. Freudenberger, J. Furrer, H. Kessler, B. Luy, *J. Magn. Reson.* **2008**, *192*, 314.

[19] S. Immel, M. Köck, M. Reggelin, *Chem. A Eur. J.* **2018**, *24*, 13918.

[20] a) J. A. Losonczi, M. Andrec, M. W. F. Fischer, J. H. Prestegard, *J. Magn. Reson.* **1999**, *138*, 334; b) G. H. Golub, C. Reinsch, *Numer. Math.* **1970**, *14*, 403.

[21] Y. Liu, R. D. Cohen, G. E. Martin, R. T. Williamson, *J. Magn. Reson.* **2018**, *291*, 63.

[22] a) C. M. Thiele, V. Schmidts, B. Böttcher, I. Louzao, R. Berger, A. Maliniak, B. Stevensson, *Angew. Chem. Int. Ed.* **2009**, *48*, 6708; b) H. Sun, U. M. Reinscheid, E. L. Whitson, E. J. d'Auvergne, C. M. Ireland, A. Navarro-Vázquez, C. Griesinger, *J. Am. Chem. Soc.* **2011**, *133*, 14629; c) E. E. Burnell, C. A. de Lange, *J. Magn. Reson.* **1980**, *39*, 461.

[23] B. Nieto-Ortega, R. Rodriguez, S. Medina, E. Quinoa, R. Riguera, J. Casado, F. Freire, F. J. Ramirez, *J. Phys. Chem. Lett.* **2018**, *9*, 2266.

[24] a) P. Mukhopadhyay, G. Zuber, P. Wipf, D. N. Beratan, *Angew. Chem. Int. Ed.* **2007**, *46*, 6450; b) F. Egidi, T. Giovannini,

G. Del Frate, P. M. Lemler, P. H. Vaccaro, C. Cappelli, *Phys. Chem. Chem. Phys.* **2019**, *21*, 3644.
[25] A. Meddour, D. Atkinson, A. Loewenstein, J. Courtieu, *Chem.--Eur. J.* **1998**, *4*, 1142.
[26] C. Fehr, I. Magpantay, M. Vuagnoux, P. Dupau, *Chem. A Eur. J.* **2011**, *17*, 1257.

SUPPORTING INFORMATION

Additional supporting information may be found online in the Supporting Information section at the end of this article.

How to cite this article: Krupp A, Noll M, Reggelin M. Valine derived poly (acetylenes) as versatile chiral lyotropic liquid crystalline alignment media for RDC-based structure elucidations. *Magn Reson Chem*. 2021;59:577–586. https://doi.org/10.1002/mrc.5003